Theoretical Demonstration of How the Dispersion of Magnetic Excitations in Cuprate Compounds can be Determined Using Resonant Inelastic X-Ray Scattering

Luuk J. P. Ament,[1,4] Giacomo Ghiringhelli,[2] Marco Moretti Sala,[2] Lucio Braicovich,[2] and Jeroen van den Brink[1,3,4]

[1]Institute-Lorentz for Theoretical Physics, Universiteit Leiden, 2300 RA Leiden, The Netherlands
[2]INFM/CNR Coherentia and Soft-Dipartimento di Fisica, Politecnico di Milano, Piazza Leonardo da Vinci 32, 20133 Milano, Italy
[3]Institute for Molecules and Materials, Radboud Universiteit, 6500 GL Nijmegen, The Netherlands
[4]Stanford Institute for Materials and Energy Sciences, Stanford University and SLAC National Accelerator Laboratory, Menlo Park, California 94025, USA

(Received 13 March 2009; published 11 September 2009)

We show that in resonant inelastic x-ray scattering (RIXS) at the copper L and M edge direct spin-flip scattering is in principle allowed. We demonstrate how this possibility can be exploited to probe the dispersion of magnetic excitations, for instance magnons, of cuprates such as the high T_c superconductors. We compute the relevant local and momentum dependent magnetic scattering amplitudes, which we compare to the elastic and dd-excitation scattering intensities. For cuprates these theoretical results put RIXS as a technique on the same footing as neutron scattering.

DOI: 10.1103/PhysRevLett.103.117003 PACS numbers: 74.25.Jb, 74.72.−h, 75.25.+z, 78.70.Ck

Introduction.—In recent years the experimental technique of resonant inelastic x-ray scattering (RIXS) has made tremendous progress in terms of energy and momentum resolution [1–10]. RIXS is particularly apt to probe the properties of strongly correlated electrons, for instance in transition metal oxides. With an incoming x ray of energy $\omega_{\rm in}$ first an electron is resonantly excited from a core level into the valence shell. Subsequently, one measures the energy $\omega_{\rm out}$ of the outgoing x ray resulting from the recombination of the core hole with a valence electron. Depending on the resonance that the experiment is performed at, $\omega_{\rm in}$ corresponds to the transition metal K edge ($1s \rightarrow 4p$), L edge ($2p \rightarrow 3d$) or M edge ($3p \rightarrow 3d$). Compared to x-ray photon spectroscopies, RIXS has the advantage that there is no core hole present in the final state, so that the energy and momentum lost by the scattered photon is directly related to electronic excitations within the strongly correlated $3d$ valence bands. The chemical selectivity and bulk sensitivity of RIXS allows the study of the electronic and magnetic properties of, for example, nanostructured materials, inaccessible with nonresonant techniques.

Here we show that contrary to common belief [9–12], RIXS at the copper L edge is also a powerful probe of single-spin-flip excitations and related magnetic dispersions. The presence of this magnetic scattering channel is an important theoretical result because it puts L edge RIXS on, for instance, the high-T_c superconductors, as a technique on the same footing as neutron scattering.

Soft x-ray RIXS has been much used in transition metal oxides to study local transitions, such as dd excitations in cuprates [2,9,10] and spin flips [3,4] in NiO. Although interesting in themselves, these experiments do not exploit a unique capability of RIXS: to measure the *dispersion* of excitations by determining both momentum change and energy loss of the scattered x-ray photons. This capability is far beyond the possibilities of traditional low energy optical techniques, which are constrained to essentially zero momentum transfer because, as opposed to high energy x rays, photons in the visible range carry negligible momentum. This asset of RIXS has already been exploited to determine the momentum dependence of charge [6,7], bimagnon [8,13–15] and orbital excitations [16] at Cu K and L_3 edges.

In order to proof that at the Cu L edge RIXS can probe the dispersion of collective magnetic excitations, we will first determine the local spin-flip cross section for a copper d^9 ion in a tetragonal crystal field. This is the familiar case encountered in numerous cuprates, with one hole occupying the x^2-y^2 orbital. The important observation is that the local spin-flip process can either be forbidden or allowed, depending on the spatial orientation of the copper spin. Subsequently, we calculate the momentum ($\mathbf{q}$-) dependence of the magnon cross section for a spin system with a collective response. As an example, we consider the Heisenberg antiferromagnet, where we find a vanishing of the magnon scattering intensity around the center of the brillouin zone proportional to $|\mathbf{q}|$ and a strong peak at the antiferromagnetic wave vector.

Local spin-flip scattering at Cu L edge.—From the viewpoint of inelastic magnetic scattering, RIXS and neutron scattering appear to be very different techniques. It is easy to show, for instance, that in transition metal K edge RIXS single-spin-flip scattering is forbidden [13] because of the absence of spin-orbit coupling in the intermediate state. Ever since the seminal work of Kuiper and co-workers [9], more than a decade ago, it is believed that also at the copper L and M edge spin-flip scattering is not allowed for Cu^{2+} in a tetragonal crystal field, unless the spin-flip excitation is accompanied by a dd excitation [10–12].

Based on a symmetry analysis of the wave function of the copper hole, Ref. [11] concludes that "the x^2-y^2 state, a linear combination of atomic $Y_{2,2}$ and $Y_{2,-2}$ states, does not allow a direct spin-flip transition." The observation that the spin-flip excitations are intrinsically entangled with *dd* excitations implies that mapping out momentum dependencies of magnetic excitations with L edge RIXS would be a hopeless endeavor. As will be clarified shortly, the *dd* excitations act as a momentum sink, which would limit the information that can be gained from RIXS to *momentum averaged properties* of the magnetic excitations, preempting the possibility to observe, e.g., a single magnon dispersion.

We show in the following, however, that the symmetry analysis on which these assertions rely [10,11] is incomplete because it is restricted to directions of the spin moment along an axis that is orthogonal to the x^2-y^2 orbital. In fact, we will show that for any other spin orientation direct spin-flip scattering is allowed. This includes, in particular, Néel ordered cuprates, where the magnetic moment lies in the plane of the x^2-y^2 orbital: for example, in La_2CuO_4, $Sr_2CuO_2Cl_2$, and $(CaSr)CuO_2$ [17,18], spins order along the $[x, y, z] = [110]$ direction and in Nd_2CuO_4 along [100] and [010] in alternating planes [19].

The dependence of the direct spin-flip scattering amplitude on photon polarization, scattering angle and momentum transfer can be computed from the Kramers-Heisenberg expression [20]: $A_{fi} \propto \sum_n \langle f|\hat{D}|n\rangle\langle n|\hat{D}|i\rangle / (\omega_{\rm det} - E_n + i\Gamma)$, where A_{fi} is the scattering amplitude from initial state i to final state f, $\hat{D}$ the polarization dependent dipole operator, $\omega_{\rm det} \equiv \omega_{\rm in} - \omega_{\rm res}$ is the detuning away from the resonance energy $\omega_{\rm res}$ ($\sim$930 eV at the copper L_3 edge), $|n\rangle$ the intermediate state with energy E_n (measured with respect to the resonance energy) and Γ the core-hole lifetime. At the copper L edge we are dealing with the local electronic process $2p^6 3d^9 \rightarrow 2p^5 3d^{10} \rightarrow 2p^6 3d^{9*}$, where $*$ denotes an excited state with a *dd* excitation and/or spin flip. At the L_3 resonance the intermediate states $|n\rangle$ are just the multiplets corresponding to the four $J^z = L^z + S^z$ states of the spin-orbit coupled $2p_{3/2}$ core hole.

It is easy to see that direct spin-flip excitations are forbidden if the spin of the hole in the x^2-$y^2 = (Y_{2,2} + Y_{2,-2})/\sqrt{2}$ initial state is aligned along [001], which is the situation considered previously [10,11]. In the first step of the RIXS process a dipole allowed $2p \rightarrow 3d$ transition creates a core hole in a linear combination of $Y_{1,1}$ and $Y_{1,-1}$, while conserving the spin. In this intermediate state the spin-orbit coupling of the core hole $\mathbf{L} \cdot \mathbf{S} = L^z S^z + (L^+ S^- + L^- S^+)/2$ can cause a spin flip S^- (or S^+) in combination with a raising (or lowering) L^+ (or L^-) of the orbital moment. In either case a $Y_{1,0}$ core-hole state with reversed spin is the result [10,11,21]. The last step to end up in a final state with only a spin-flip excitation, requires the optical decay of the $Y_{1,0}$ $2p$ core hole into a $(Y_{2,2} + Y_{2,-2})/\sqrt{2}$ $3d$ valence band hole. This transition is dipole forbidden because it requires $\Delta L^z = 2$, which thus forbids direct spin-flip scattering.

The situation changes drastically when the local magnetic moment is oriented in the x-y plane: we will show that in this case direct spin-flip excitations are fully allowed. This is best illustrated by a direct calculation of the RIXS amplitudes in the different channels for Cu^{2+} in a tetragonal crystal field. We consider a scattering geometry as in Fig. 1(a), with fixed scattering angle of 90° and π (σ) linear polarization of the incident photons parallel (perpendicular) to the scattering plane. In this geometry $\theta_{\rm IN}$ is the azimuthal angle between incident beam and [001] axis. In Fig. 1(b) we show the polarization and momentum

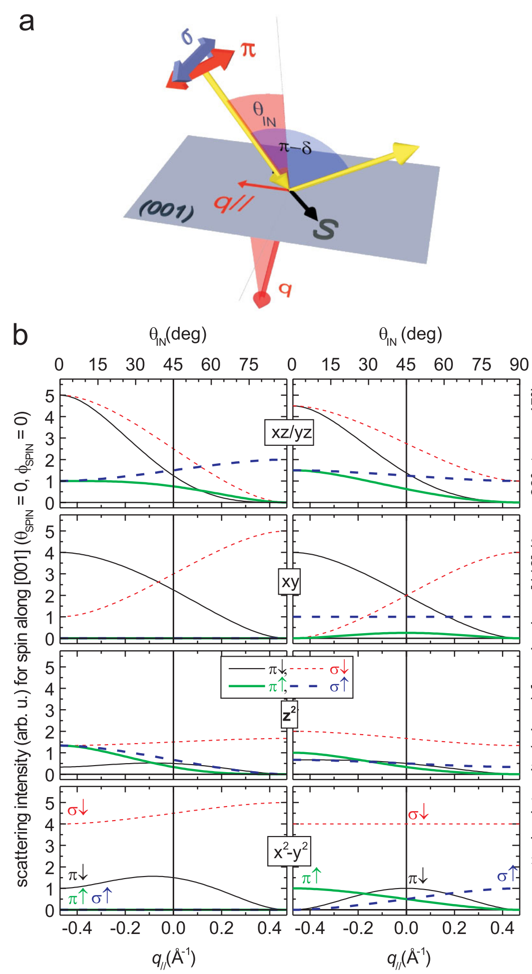

FIG. 1 (color online). L_3 RIXS cross section for a single Cu^{2+} ion with σ and π polarization of the incident beam. (a) The geometry: the scattering plane is (100), scattering angle 90°, the incident photons impinge at an angle $\theta_{\rm IN}$ to the [001] direction (c axis). (b) Scattering intensities to different orbital and spin orientations, starting from a $(x^2$-$y^2) \downarrow_z$ state (left panels) and a $(x^2$-$y^2) \downarrow_{xy}$ ground state (right panels) as a function of $\theta_{\rm IN}$ or alternatively the in-plane transferred momentum $q_{\parallel}$. For $\downarrow_z$, i.e., spin along [001], the spin-flip cross section vanishes (bottom left), not so for $\downarrow_{xy}$, with spin along [110] (right).

dependent RIXS matrix elements to all possible final states for the starting configuration of a hole in the x^2-y^2 orbital with a spin oriented either along [001] (left panels) or along [110] (right panels), denoted by $(x^2\text{-}y^2)\downarrow_z$ and $(x^2\text{-}y^2)\downarrow_{xy}$, respectively, so that $(x^2\text{-}y^2)\uparrow$ is a final state with only a spin-flip excitation.

Note that along the [100] direction the nuclear Brillouin zone boundary is at $q_{\parallel} \approx 0.826\hbar$ Å^{-1} for $a = 3.8$ Å, an in-plane lattice parameter that is typical for cuprates. At 90° scattering Cu L_3 RIXS can explore half of the reciprocal space, but going to backscattering geometry $q_{\parallel}$ grows considerably and almost all the Brillouin zone can be covered. Figure 1(b) shows that the spin flip to *dd* excitation intensity ratio varies from zero at the zone-center to about 0.1 at the zone edge. From the lower panels in Fig. 1 at the left and right it is clear that for a spin along [110] the spin-flip cross section is allowed for both σ and π polarizations, whereas it is in all cases forbidden for a spin along [001]. It is interesting to note that for the σ polarization the elastic peak is more than 4 times stronger than the spin-flip scattering channel, whereas for π the two intensities are similar. The direct spin-flip cross section for a generic spin direction, characterized by the Euler angles (θ_{spin}, ϕ_{spin}) is shown in Fig. 2 for a number of azimuthal angles θ_{IN}.

The upshot of these numerical results can easily be understood on the basis of a symmetry argument. If the spin of the x^2-y^2 hole points along the x axis, it is in the spin state $(|\uparrow\rangle + |\downarrow\rangle)/\sqrt{2}$, corresponding to $S^x = 1/2$. In the intermediate $2p_{3/2}$ core-hole state the diagonal part of the spin-orbit coupling, $L^z S^z$, causes a transition of this spin state into $(|\uparrow\rangle - |\downarrow\rangle)/\sqrt{2}$ (corresponding to $S^x = -1/2$), while the angular part of the core-hole wave function stays in a linear combination of $Y_{1,1}$ and $Y_{1,-1}$. The transition of the core-hole back into the $3d$ x^2-y^2 orbital is therefore dipole allowed while at the same time the spin along the x axis is flipped.

Momentum dependence of magnon cross section.—We now wish to generalize the cross section from local spin flips to collective magnetic excitations, which are characterized by their momentum quantum number $\mathbf{q}$. There are several ways to compute the $\mathbf{q}$ dependence of this cross section, but a particularly transparent one is by expanding the Kramers-Heisenberg scattering amplitude formally in a power series of the intermediate state Hamiltonian H_{int}: $A_{fi} = \sum_{l=0}^{\infty} \langle f|\hat{D}(H_{\text{int}})^l \hat{D}|i\rangle/\Delta^{l+1}$, with $\Delta = \omega_{\text{det}} + i\Gamma$, which is the starting point for the ultrashort core-hole lifetime expansion for RIXS [15,22,23]. The dipole operator $\hat{D} = \hat{D}_0 + \hat{D}_0^{\dagger}$, now allows for a direct creation of a spin flip upon deexcition. The corresponding amplitude r_{ϵ} depends on incident and outgoing polarization (ϵ and ϵ' respectively), as clarified above and shown in Figs. 1 and 2. We thus obtain

$$\hat{D}_0(\epsilon, \epsilon') = \sum_i r_{\epsilon'} S_i^z e^{i\mathbf{q}_{\text{out}}\cdot\mathbf{R}_i} d_i^{\dagger} p_i + r_{\epsilon} e^{-i\mathbf{q}_{\text{in}}\cdot\mathbf{R}_i} p_i^{\dagger} d_i,$$

where $d_i^{\dagger}$ and $p_i^{\dagger}$ create a $3d$ valence hole and $2p$ core-hole, respectively. The operator S^z flips the spin when it is in the xy plane. In the operator $\hat{D}_0$ all magnetic effects of the intermediate state core-hole Hamiltonian have been taken into account so that the RIXS amplitude becomes $A_{fi} = r_{\epsilon} r_{\epsilon'} \langle f|\sum_i e^{i\mathbf{q}\cdot\mathbf{R}_i} S_i^z|i\rangle/\Delta$ with $\mathbf{q} = \mathbf{q}_{\text{out}} - \mathbf{q}_{\text{in}}$. The inelastic magnetic scattering amplitude finally reduces to $A_{fi} = r_{\epsilon} r_{\epsilon'} \langle f|S_{\mathbf{q}}^z|i\rangle/\Delta$.

It is instructive to compute with this generic expression the single magnon RIXS spectrum for an antiferromagnetic 2D Heisenberg model, given by the Hamiltonian $H = J\sum_{\langle ij\rangle} \mathbf{S}_i \cdot \mathbf{S}_j$. Introducing Holstein-Primakoff bosons ($S_i^x \mapsto 1/2 - a_i^{\dagger} a_i$ etc.) and adopting linear spin wave theory one finds after a Fourier and a Bogoliubov transformation the magnon scattering amplitude $\sqrt{N/2}(u_{\mathbf{q}} - v_{\mathbf{q}})\langle f|\alpha_{\mathbf{q}} + \beta_{\mathbf{q}} + \alpha_{-\mathbf{q}}^{\dagger} + \beta_{-\mathbf{q}}^{\dagger}|i\rangle/\Delta$ with N the total number of sites and the Bogoliubov transformed boson operators $\alpha_{\mathbf{k}} = u_{\mathbf{k}} a_{\mathbf{k}} + v_{\mathbf{k}} b_{-\mathbf{k}}^{\dagger}$ and $\beta_{\mathbf{k}} = u_{\mathbf{k}} b_{\mathbf{k}} + v_{\mathbf{k}} a_{-\mathbf{k}}^{\dagger}$. The resulting zero-temperature single magnon spectrum is shown in Fig. 3. At $\mathbf{q} = (0, 0)$ the magnon scattering amplitude vanishes because in this situation the scattering

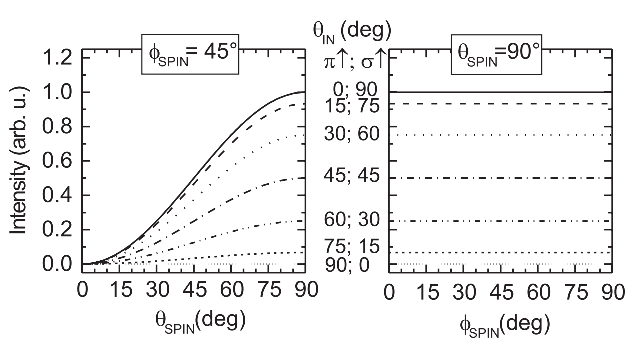

FIG. 2. The dependence of scattering cross section for spin-flip scattering to $(x^2\text{-}y^2)\uparrow$ final states on the atomic spin orientation for selected cases of scattering geometry given by varying θ_{IN} and fixed $\phi_{\text{IN}} = 0$.

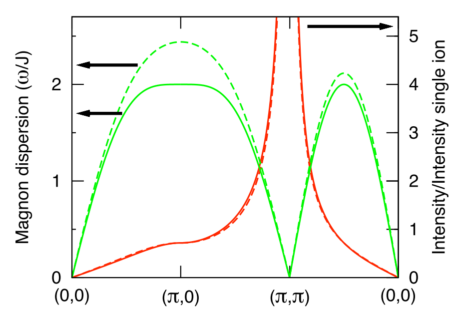

FIG. 3 (color online). Momentum dependence of the magnetic RIXS spectral weight at the copper L_3 edge (red) and the magnon dispersion (green) for a simple 2D Heisenberg model (solid lines) and an extended model relevant for La_2CuO_4 [24] (dashed).

operator is proportional to the total spin in the z-direction $S^z_{\rm tot}$, which does not cause inelastic processes. For small transferred momenta, $|\mathbf{q}| \to 0$, the magnon scattering intensity vanishes as $\omega_{\mathbf{q}}/4J$. We also observe that the magnon cross section diverges at $\mathbf{q} = (\pi, \pi)$ as $4J/\omega_{\mathbf{q}}$, similar to the neutron scattering form factor. This divergence is due to the RIXS photons scattering on spin fluctuations: at $\mathbf{q} = (\pi, \pi)$ the scattering operator is proportional to the staggered spin along the z axis $S^z_{\rm stag}$, so that the total, energy integrated, scattering intensity $\int d\omega \sum_f |A_{fi}|^2 \delta(\omega - \omega_{fi}) \propto \langle (S^z_{\rm stag})^2 \rangle$ and the inelastic scattering intensity is proportional to the variance $\langle (S^z_{\rm stag})^2 \rangle - \langle S^z_{\rm stag} \rangle^2$. We performed the same calculation for a Hamiltonian including longer-range and ring exchange terms, with a parameterization derived from neutron scattering [24]. Figure 3 shows that these additional interactions cause only small changes in the momentum dependence of the magnetic scattering cross section.

Using the same formalism, we can compute the $\mathbf{q}$ dependent scattering amplitude of a spin-flip entangled with a dd excitation. If the local spin-flip operator is S_i^- and the operator corresponding to the dd transition is T_i^+, the inelastic scattering amplitude is $A_{fi} \propto \langle f | \sum_i e^{i\mathbf{q}\cdot\mathbf{R}_i} S_i^- T_i^+ | i \rangle = \langle f | \sum_{\mathbf{k}} S^-_{\mathbf{k}} T^+_{\mathbf{k}-\mathbf{q}} | i \rangle$. Clearly part of the momentum is absorbed by the dd excitation, so that RIXS measures a momentum convolution of the two excitations. In particular, the magnetic scattering amplitude looses all $\mathbf{q}$ dependence if the dd excitation is dispersionless, exemplifying that in order to determine magnon dispersions the presence of a *direct* spin-flip process is essential.

Conclusions.—Depending on the spatial orientation of the copper spin, local spin-flip process for RIXS at the L_3 edge can be forbidden or allowed. This makes RIXS a very sensitive probe of the orientation of the local magnetic moment. In typical cuprates direct spin-flip scattering is allowed and for this case we determined the spin-flip and magnon cross section, which turns out to be strongly momentum and polarization dependent. Our theory holds at both the copper L and M edges. At the M edge ($\omega_{\rm in} \approx$ 75 eV) the photon momentum is small, so that only magnons in a very small portion of the Brillouin zone can be probed. But at the copper L_3 edge the x-ray photon carries a momentum $|\mathbf{q}_{\rm in}| \sim 0.47\hbar$ Å^{-1}, which is in a typical cuprate large enough to observe magnetic excitations in almost all of the Brillouin zone. Indeed very recently high resolution soft x-ray RIXS experiments on La_2CuO_4 have for the first time resolved the single magnon dispersion, confirming the predictions of this Letter [25]. Thus, at least for high-T_c superconductors, L edge RIXS can be placed on the same footing as neutron scattering—with the additional great advantage that for photon scattering only small sample volumes are required so that the measurement of the spin dynamics of thin films, oxide heterostructures and other nanostructures now comes within experimental reach.

We thank Michel van Veenendaal, Tom Devereaux, Maurits Haverkort, Marco Grioni, and George Sawatzky for stimulating discussions. This research benefited from the RIXS collaboration supported by the Computational Materials Science Network (CMSN) program of the Division of Materials Science and Engineering, U. S. Department of Energy, Grant No. DE-FG02-08ER46540 and is supported by the Dutch Science Foundation FOM.

[1] W. Schülke, *Electron Dynamics by Inelastic X-Ray Scattering* (Oxford University Press, Oxford, 2007).
[2] G. Ghiringhelli *et al.*, Phys. Rev. Lett. **92**, 117406 (2004).
[3] S. G. Chiuzbăian *et al.*, Phys. Rev. Lett. **95**, 197402 (2005).
[4] G. Ghiringhelli *et al.*, Phys. Rev. Lett. **102**, 027401 (2009).
[5] L. Braicovich *et al.*, Phys. Rev. Lett. **102**, 167401 (2009).
[6] M. Z. Hasan *et al.*, Science **288**, 1811 (2000).
[7] Y. J. Kim *et al.*, Phys. Rev. Lett. **89**, 177003 (2002).
[8] J. P. Hill *et al.*, Phys. Rev. Lett. **100**, 097001 (2008).
[9] P. Kuiper *et al.*, Phys. Rev. Lett. **80**, 5204 (1998).
[10] M. A. van Veenendaal, Phys. Rev. Lett. **96**, 117404 (2006).
[11] F. M. F de Groot, P. Kuiper, and G. A. Sawatzky, Phys. Rev. B **57**, 14 584 (1998).
[12] A. Kotani and S. Shin, Rev. Mod. Phys. **73**, 203 (2001).
[13] J. van den Brink, Europhys. Lett. **80**, 47003 (2007).
[14] T. Nagao and J. I. Igarashi, Phys. Rev. B **75**, 214414 (2007).
[15] F. Forte, L. J. P. Ament, and J. van den Brink, Phys. Rev. B **77**, 134428 (2008).
[16] F. Forte, L. J. P. Ament, and J. van den Brink, Phys. Rev. Lett. **101**, 106406 (2008).
[17] D. Vaknin *et al.*, Phys. Rev. Lett. **58**, 2802 (1987).
[18] D. Vaknin *et al.*, Phys. Rev. B **39**, 9122 (1989).
[19] S. Skanthakumar *et al.*, Physica (Amsterdam) **160C**, 124 (1989).
[20] M. Blume, J. Appl. Phys. **57**, 3615 (1985).
[21] M. van Veenendaal (private communication).
[22] J. van den Brink and M. van Veenendaal, Europhys. Lett. **73**, 121 (2006).
[23] L. J. P. Ament, F. Forte, and J. van den Brink, Phys. Rev. B **75**, 115118 (2007).
[24] R. Coldea *et al.*, Phys. Rev. Lett. **86**, 5377 (2001): next-nearest neighbor $J'/J = -0.11$, next-next-nearest neighbor $J''/J = 0.026$ and ring exchange $J_\square/J = 0.41$.
[25] L. Braicovich *et al.* (unpublished).